A Microfluidic Device Integrating a Glucose Sensor and Calibration Function for Cell-Based Assays

Laner Chen , Kenta Shinha , Hiroko Nakamura , Kikuo Komori , Hiroshi Kimura *

Posted Date: 8 April 2025

doi: 10.20944/preprints202504.0616.v1

Keywords: microfluidic system; microphysiological system (MPS); biosensor; glucose oxidase; calibration; cell-based assay; paraquat

 doi:10.20944/preprints202504.0616.v1

Article

A Microfluidic Device Integrating a Glucose Sensor and Calibration Function for Cell-Based Assays

Laner Chen [1], Kenta Shinha [2], Hiroko Nakamura [2], Kikuo Komori [3] and Hiroshi Kimura [1,2,*]

[1] Department of Mechanical Engineering, School of Engineering, Tokai University, Kitakaname, Hiratsuka 259-1292, Kanagawa, Japan

[2] Micro/Nano Technology Center, Tokai University, Kitakaname, Hiratsuka 259-1292, Kanagawa, Japan

[3] Department of Biotechnology and Chemistry, Faculty of Engineering, Kindai University, Takaya-Umenobe, Higashi-Hiroshima 739-2116, Hiroshima, Japan

* Correspondence: Hiroshi Kimura, hkimura@tokai.ac.jp

Abstract: Microphysiological systems (MPS) incorporating microfluidic technologies offer improved physiological relevance and real-time analysis for cell-based assays, but often lack non-invasive monitoring capabilities. Addressing this gap, we developed a microfluidic cell-based assay platform integrating an electrochemical biosensor for real-time, non-invasive monitoring of kinetic cell status through glucose consumption. The platform addresses the critical limitations of traditional cell assays, which typically rely on invasive, discontinuous methods. By combining enzyme-modified platinum electrodes within a microfluidic device, our biosensor can quantify dynamic changes in glucose concentration resulting from cellular metabolism. We have integrated a calibration function that corrects sensor drift, ensuring accurate and long-term measurement stability. In validation experiments, the system successfully monitored glucose levels continuously for 20 h, demonstrating robust sensor performance and reliable glucose concentration predictions. Furthermore, in cell toxicity assays using HepG2 cells exposed to varying concentrations of paraquat, the platform detected changes in glucose consumption, effectively quantifying cellular toxicity responses. This capability highlights the device's potential for accurately assessing the dynamic physiological conditions of cells. Overall, our integrated platform significantly enhances cell-based assays by enabling continuous, quantitative, and non-destructive analysis, positioning it as a valuable tool for future drug development and biomedical research.

Keywords: microfluidic system; microphysiological system (MPS); biosensor; glucose oxidase; calibration; cell-based assay; paraquat

1. Introduction

In recent years, the microphysiological system (MPS), which combines microfluidic device technology with cell culture and assay approaches, has been considered an ideal approach for cell analysis in drug development and research [1–5]. Compared to traditional cell research approaches, these platforms are recognized for their numerous advantages, including more physiologically relevant cell culture conditions and efficient cell assay methods. For example, perfusion of culture medium in these platforms can contribute to the delivery of nutritional supplements and simulate shear stress loading on cells, thereby mimicking in vivo conditions [6,7]. However, cell status measurement in previous MPSs is still challenging because traditional methods, such as cell staining and imaging, inevitably cause irreversible damage to cells. The obtained optical or quantified data are discrete, allowing for the analysis of real-time changes in cell status. Thus, the non-invasive and real-time quantified cell status analysis system is expected to be advanced in MPSs.

There has been intensive research in medical diagnostics aimed at developing a reliable cell analysis platform that integrates biosensors to monitor the in vitro transient fluxes involved in

 doi:10.20944/preprints202504.0616.v1

cellular metabolism under exposure to medical materials. Monitoring changes in the levels of key substances, such as oxygen, glucose, and lactate, facilitates the quantification of cell growth and proliferation rates through the cell's glucose metabolism [8–10]. Electrochemical biosensors, which utilize oxidation-reduction reactions and measure the response current, are effective electronic components and have been widely applied to analyze bioactive samples. In many previous studies, biological recognition element-casting electrodes, such as those using glucose oxidase (GOD), have been widely employed in electrochemical analysis under cell culture conditions due to their ability to detect certain substances [11–13]. In the section on electrode materials, platinum (Pt) is considered a better electrode material, contributing to higher sensitivity, resolution, and longer lifetime, which improves the performance of existing enzyme-modified electrodes compared to gold (Au) [14]. Combination enzyme-modified electrodes, along with conventional reference and counter electrodes, are expected to serve as biosensors for monitoring changes in physiological conditions in cell-based experiments [15].

These cell-based analysis platforms, which integrate electrochemical biosensors into microfluidic devices, are expected to monitor in vitro dynamic cell state changes under in vivo conditions mimicking [16]. With advances in existing devices that integrate biosensors, microfluidic devices obtained by photolithographic and planar techniques can be utilized due to certain advantages, such as sample holding and microfluidic flow control. These advantages enabled it to measure low sample volumes with higher sensitivity and faster response times. Additionally, the flow rate control and injection solution control at these microfluidic devices enable real-time adjustment of diffusion layers, allowing for the adaptation of the sensor's sensitivity and linear responses. However, electrochemical sensor drift resulting from a decrease in enzyme activity leads to an uncertain prediction of analyte levels, limiting the platform to short-term monitoring only.

Some previous studies have reported comparing the status of cells under toxic conditions with that under non-toxic conditions to determine the changes in cell kinetic status under toxic conditions [17]. The other study reported that the cells' glucose consumption varied between upstream and downstream glucose concentrations [18]. However, more than one sensor's measurement result was discussed in these studies, which led to uncertain predictions because of individual differences in sensors or cells. Thus, online sensor calibration focusing on one single sensor is expected to improve the lifetime and measurement stability of enzyme-modified biosensors in long-term monitoring.

In this study, we report on a cell-based assay platform featuring an integrated electrochemical glucose sensor designed to monitor kinetic changes in cell status during toxicity experiments. For certain predictions of glucose concentration and standalone cell analysis, the calibration function was integrated into the microfluidic device for recalibration of the biosensor. We evaluate the biosensor's basic measurement function and the microfluidic device's calibration function in a long-term measurement experiment. Then, we monitored the cell kinetic status through glucose consumption during a cell-based toxicological experiment to assess the performance of the cell-based assay platform.

2. Materials and Methods

2.1. Cell-Based Assay Platform

We developed a cell-based assay platform that incorporates a microfluidic device with an enzyme-modified biosensor, that was connected to syringe pumps and a potentiostat, for monitoring the dynamic state of cells (Figure 1A). The microfluidic device was fabricated by assembling a dimethylpolysiloxane (PDMS) chip with microchannel structures and a glass substrate with electrodes for an enzyme-modified biosensor.

2.2. PDMS Chip

The microfluidic chip had a cell culture chamber, a biosensor chamber, and microfluidic channels. The biosensor chamber was modulated downstream of the cell culture chamber (Figure

 doi:10.20944/preprints202504.0616.v1

1B). The calibration solutions inlet A (for low glucose concentration solutions) and the calibration solutions inlet B (for high glucose concentration solutions) were sitting near the main inlet of the sensor chamber. Three microfluidic channels of the inlets collapsed at the upper stream of the biosensor chamber. The cell culture chamber was designed with a height of 500 μm and a culture area of 530 mm^2. Six pillars (diameter 2 mm) were uniformly situated in the cell-culture chamber to prevent the attachment of the upper and bottom surfaces during the fabrication process. The biosensor chamber was designed with a height of 90 μm and a width of 3 mm (Figure 1C). The two chambers' different heights and cross-sectional areas were designed to allow for less shear stress loading at the cell culture chamber, maintaining a constant flow rate [19].

The microfluidic chip was fabricated through conventional PDMS replica molding processes, and the negative pattern mold for the microfluidic chip was also created using a conventional photolithography process with negative photoresist SU-8 [20]. However, the SU-8 mold fabrication required two photolithography processes to build different thickness photoresist layers on a single Si wafer. A Si wafer cleaned with a piranha solution (a mixture of hydrogen peroxide (18084-00, KANTO KAGAKU, Tokyo, Japan) and sulfuric acid (37390-00, KANTO KAGAKU, Tokyo, Japan)) and coated with BHF was spin-coated at 1800 rpm with a layer of photoresist SU-8 2075 (Y111074, Nippon Chemical Industrial, Tokyo, Japan). The wafer was then exposed to UV light to obtain a template of the microchannel channels and sensor chamber with a thickness of 90 μm. The same photolithography process was conducted using SU-8 2100 (Y111075, Nippon Chemical Industrial, Tokyo, Japan) and a spin-coating speed of 800 rpm to obtain a mold of the culture chamber with a thickness of 500 μm. The position of the photo mask was adjusted using the microscope to align the attachment marks before UV exposure. The completed template was treated with CHF3 plasma (RIE-10NR, Samco, Kyoto, Japan) to deposit a fluorocarbon layer onto the surface of the SU-8 mold, ensuring the easy release of PDMS chips from the SU-8 mold.

The liquid-state PDMS (0008494274, Dow Corning Toray, Michigan, USA) was poured into the SU-8 mold, and the bubbles were removed in a vacuum chamber. After 1 h and 30 min baking at 70 ℃, the PDMS chip was hardened and ready to peel off from the SU-8 mold. Holes were made at all inlets and outlets using a biopsy punch (BP-40F, Kai Medical, Gifu, Japan), and these were connected to syringe pumps or medium reservoirs using silicone tubes (Figure 1A).

 doi:10.20944/preprints202504.0616.v1

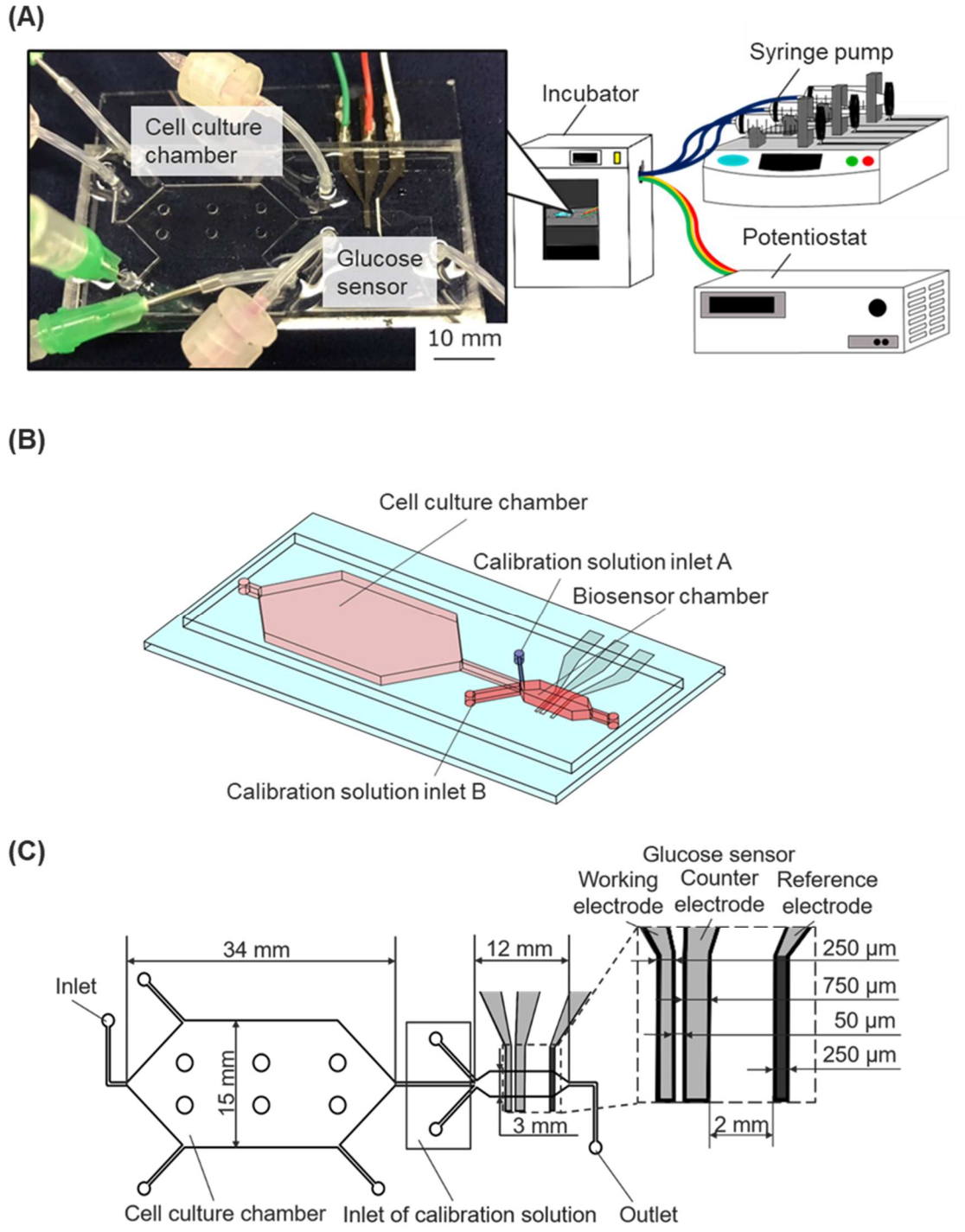

Figure 1. The cell-based assay platform consists of a microfluidic device with a glucose biosensor, a fluidic system, and a potentiostat. (A) Experimental setup: The microfluidic device, connected to syringe pumps and a potentiostat, was installed in an incubator. (B) Schematic image of the microfluidic device. (C) The geometry of the microfluidic device with the integrated glucose sensor.

2.3. Enzyme-Modified Biosensor

The Pt electrodes on the glass structure were modified with glucose oxidase (GOD) to function as electrochemical biosensors for measuring glucose concentration in culture media. The sensor shapes and arrangement are shown in Figure 1C. Three-electrode electrochemical biosensors, comprising a working electrode, a reference electrode, and a counter electrode, were utilized. The working electrode (width, 250 µm) was positioned at the upper stream of the chamber, the counter

 doi:10.20944/preprints202504.0616.v1

electrode (width, 750 μm) was placed after the working electrode, and the reference electrode was positioned downstream of the chamber. The conventional photolithography process fabricated the thin-film electrodes on a glass substrate, using positive photoresist masking and aqua regia for wet etching. A 50.8 mm × 76.2 mm glass substrate coated with a thin platinum film (TOA OPTICAL TECHNOLOGIES, Tokyo, Japan) was cleaned using ultrasonic cleaning and piranha solutions. It was then spin-coated with a layer of S1813G positive photoresist (10336632, ROHM and HAAS, Pennsylvania, USA). The photoresist layer was exposed to UV light using a photo mask, and then the photoresist developer modified the layer to form electrode shapes. The glass substrate was wet etched using aqua regia (a mixture of hydrochloric acid (18078-00, KANTO KAGAKU, Tokyo, Japan) and nitric acid (28161-00, KANTO KAGAKU, Tokyo, Japan)) to remove the Pt layer, thereby contributing to the shape of the Pt electrode. After wet etching, the glass structure was washed with phosphoric acid (32187-00, KANTO KAGAKU, Tokyo, Japan) and acetone.

The reference and working electrodes were treated for electrochemical measurement of glucose concentration. Initially, the reference electrode was fabricated using an Ag/AgCl ink (011464, BAS Inc., Osaka, Japan) to establish the standard potential for measurement. The GOD was coated onto the working electrode by chemical fixation. The enzyme solution was prepared by dissolving 2.5 mg GOD (G7141, Sigma-Aldrich, Massachusetts, USA) and 25 mg BSA (Bovine Serum Albumin, Sigma-Aldrich, USA) as a cross-linking agent into a 250 μL PBS(-) solution (phosphate-buffered saline, D1408, Sigma-Aldrich, Massachusetts, USA) containing 0.02% Triton X-100 (020-81155, KISHIDA CHEMICAL, Osaka, Japan), which serves as a surfactant. After the enzyme was dissolved, 15 μL of glutaraldehyde (17026-32, KANTO KAGAKU, Tokyo, Japan) was added to the enzyme solution for chemical fixation. The mixture was then vortexed to ensure sufficient fusion. A 30 μL enzyme solution was dropped onto the surface of the working electrode using a thin PDMS film mask (250 μm thick PDMS film with a 4 mm diameter hole). A 30 s spin coating at 1500 rpm was then performed to remove excess enzyme solution. The sample was stored at 4℃ for 1 h. 30 μL of 5wt% Nafion (527084, Sigma-Aldrich, Massachusetts, USA) was cast onto the surface of the sensing layer to protect it and prevent a decrease in enzyme activity due to plasma exposure during PDMS chip bonding, and was stored at 4℃ under stock conditions [21,22]. The PDMS chip was bonded onto the glass substrate with Pt electrodes via covalent bonds after oxygen plasma treatment using a plasma cleaner, resulting in a microfluidic device with an integrated glucose biosensor.

2.4. Electrochemical Measurement Principles

We first evaluated the basic performance of the Nafion/GOD-BSA/Pt electrode at a constant potential of ±0.4 V (vs. Ag/AgCl) in a 37℃ incubator and under a 9 μL/min perfusion condition to confirm the glucose concentration dependence of the biosensor. The glucose concentration range was set from 0 mM to 30 mM to maintain steady biosensor performance under normal culture conditions, encompassing the glucose concentration range between the no-glucose DMEM and high-glucose DMEM. All measurement processes were performed using an ALS/CH Instruments Electrochemical Analyzer Model ALS600B (BSA Inc., Osaka, Japan) linked to a personal computer in chronoamperometry mode. All measurements were collected at E = 0.40 V (±0.01 V) versus Ag/AgCl for glucose. The glucose concentration of measurement solutions was adjusted to 0, 0.5, 1, 2, 4, 6, 8, 10, 15, 25, and 30 mM using the no-glucose DMEM culture medium (Dulbecco's Modified Eagle's medium, 11966-025, Thermo Fisher Scientific, Massachusetts, USA) and the glucose powder (G8270, Sigma-Aldrich, Massachusetts, USA).

2.5. Long-Term Monitoring and Calibration Function

We confirmed the long-term performance of the biosensor under normal incubator conditions (37℃, 20% CO_2) and monitored glucose concentration for 20 h to evaluate the stability of the biosensor under cell culture conditions. Low-glucose DMEM (Dulbecco's Modified Eagle's medium, 12320-032, Thermo Fisher Scientific, Massachusetts, USA) containing 5.6 mM glucose has been used as an object solution.

 doi:10.20944/preprints202504.0616.v1

For calibration of the biosensor, calibration solutions containing high and low concentrations of glucose were injected into the sensor chamber intermittently, allowing for the measurement of the response current's decline over time. The linear response of the sample medium's glucose concentration was measured, and calibration processes were executed every 2 h during the usual measurement. A calibration process consists of two calibration phases: the first calibration phase and the second calibration phase (Figure 2A). Calibration solutions were prepared using low-glucose DMEM containing 10% fetal bovine serum (FBS, 10270106, Thermo Fisher Scientific, Massachusetts, USA), 25 mM HEPES, and varying glucose concentrations. In the first calibration phase, low-concentration glucose calibration solutions (containing 2 mM glucose) flowed into the biosensor chamber from inlet A for 10 min to obtain the peak value of the calibration curve. In the second calibration phase, high-concentration glucose calibration solutions (containing 8 mM glucose) flowed into the biosensor chamber from calibration solution inlet B for 10 min to obtain the foot value of the calibration curve. The fluidic control of the sample medium and calibration solutions was achieved automatically, using programming for syringe pumps to control the flow rate of each inlet (Figure 2A).

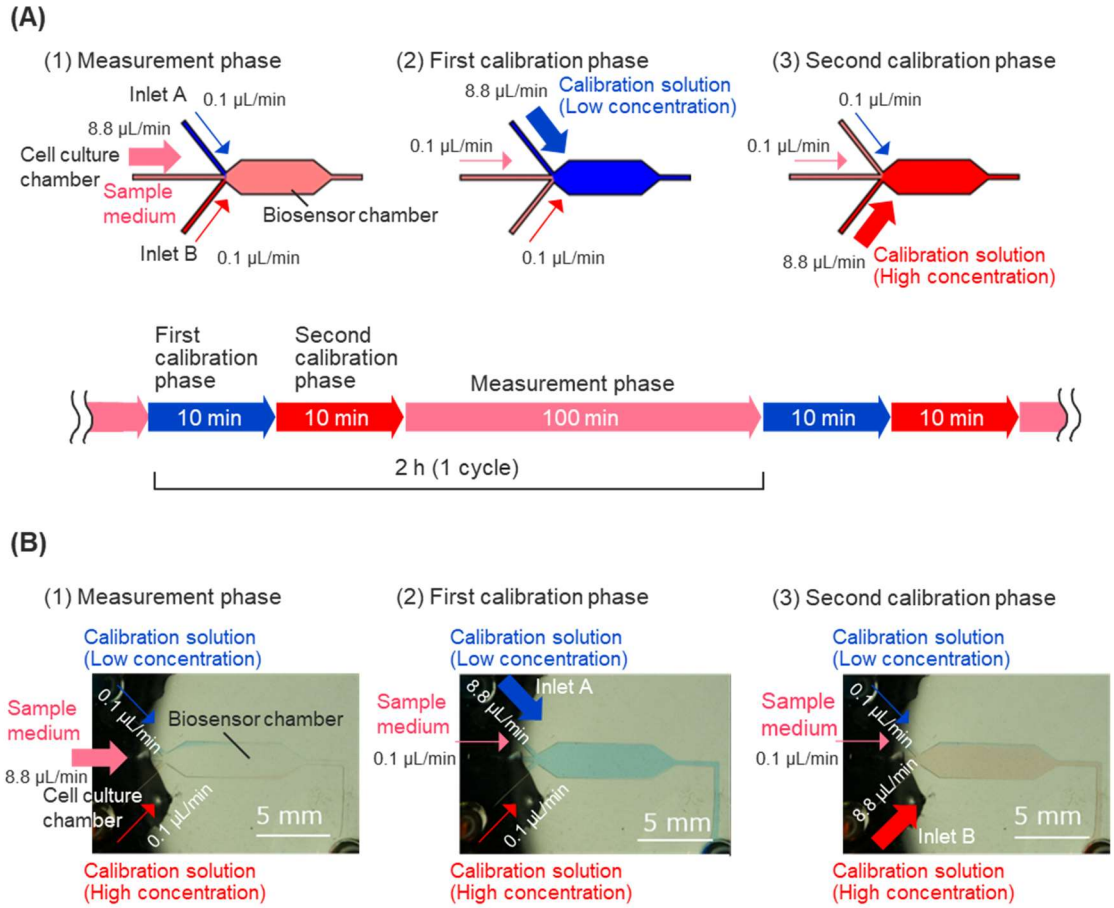

Figure 2. Automatic calibration procedure during long-term measurement. (A) During cell dynamics measurement, the sample culture medium comes from the cell culture chamber at a rate of 8.8 μL/min (1). During calibration, first, a calibration solution with a glucose concentration of 2 mM is introduced from calibration solution inlet A at a rate of 8.8 μL/min for 10 minutes (2). After that, a calibration solution with a glucose concentration of 8 mM is introduced at a rate of 8.8 μL/min from the calibration solution inlet B for 10 minutes. Through these operations, the biosensor was calibrated every 2 h during long-term measurement. (B) Laminar flow of the solutions in the biosensor chamber during calibration using colored water. To prevent backflow, two ports other than the main port were also flowed at 0.1 μL/min in each phase.

2.6. Cell Culture and Cell Toxicity Experiment

 doi:10.20944/preprints202504.0616.v1

Human hepatocarcinoma liver cells (HepG2) were obtained from ATCC (Lot58210525, HB-8065, American Type Culture Collection, Virginia, USA) and employed in experiments, employing the culture medium of low-glucose DMEM containing 10% FBS and 1% antibiotics antimycotic solution (161-23181, FUJIFILM Wako Pure Chemical Corporation, Osaka, Japan). Before cell seeding, the cell-culture chamber was injected with Cellmatrix type I-P (Collagen Type I, dissolved in diluted hydrochloric acid, 634-00663, Nitta Gelatin, Osaka, Japan) and incubated for 1 h to coat the glass substrate with collagen. The chamber was then rinsed gently twice with the following culture medium. HepG2 cells were seeded into the cell culture chamber at an optimal seeding density of 2 × 105 cells/cm^2, and the cells were allowed to stand for 24 h, ensuring the cells were attached to the base and reached a steady state.

The HepG2 cells were cultured under fluidic conditions, and the glucose concentrations of the culture medium were monitored online using the biosensor in the microfluidic device. A culture medium was injected into the cell culture chamber to provide nutritional supplements to the cells, and then flowed through the biosensor chamber to measure glucose concentration. A flow rate of 9.0 μL/min was applied during perfusion cell culture.

A toxicity assay using paraquat (DSN3228, FUJIFILM Wako Pure Chemical Corporation, Osaka, Japan) was performed to evaluate the function of our system as a cell-based platform. 0 mM, 5 mM, and 10 mM paraquat were dissolved in the following culture medium and applied in a cell toxicity experiment for 24 h. The glucose consumption (glucose concentration changes) was monitored during 24 h paraquat exposure as an index for predicting the cell's kinetic status changes. The glucose concentration's long-term measurement used the same protocol as the functional evaluation experiment (Figure 2A).

2.7. Glucose Concentration Calculation

Glucose concentrations in the long-term monitoring for evaluating calibration function and the long-term monitoring at cell toxicity experiments were calculated from calibrated current values. The response current was calibrated using a current decline rate calculated from the difference between current values in calibration processes before and after the measurement phase.

In every calibration process (*nth*), the response current values (I_{low} and I_{high}) and the calibration solutions' glucose concentrations (C_{low} and C_{high}) were used to calculate the sensitivity ($a_{calibration(n)}$, equation 1) and the estimated base current value at glucose concentration 0 mM ($I_{0(n)}$). Then, the sensitivity ($a_{calibration(n)}$) and the estimated base current value ($I_{0(n)}$) were used to establish equation 2, which expresses the relationship between the current value ($I_{calibration(n)}$) and the glucose concentration (C).

$$\boldsymbol{a_{calibration(n)} = \frac{I_{high} - I_{low}}{C_{high} - C_{low}}} \quad (1)$$

$$\boldsymbol{I_{calibration(n)} = a_{calibration(n)} \times C + I_{0(n)}} \quad (2)$$

The estimated standard current values ($I_{standard}$) at the low-glucose medium in calibration processes before (*n-1*) and after (*n*) the measurement phase was calculated based on equation 2 for prediction of current decline within the measurement phase. The current decline rate ($a_{decline(n,n-1)}$) between two calibration processes (*n* and *n-1*) was calculated using the difference between the estimated standard current values ($I_{standard(n)}$ and $I_{standard(n-1)}$) and the time in one cycle period (T=7,200 s) (equation 3).

$$\boldsymbol{a_{decline(n)} = \frac{I_{standard(n)} - I_{standard(n-1)}}{T}} \quad (3)$$

The current measured in the measurement phase (I_t) was calibrated with the current decline rate ($a_{decline(n,n-1)}$) using the following equation 4, which consists of the calibrated current value ($I_{estimated(t)}$), the response current value (I_t), the time in one cycle period (T), and measuring time in the cycle (t).

$$\boldsymbol{I_{estimated(t)} = I_t - a_{decline(n,n-1)} \times (t - T)} \quad (4)$$

Finally, the glucose concentration ($C_{estimated(t)}$) in a sample medium was calculated from calibrated current values, using the sensitivity ($a_{calibration(n)}$) and the estimated base current value ($I_{0(n)}$)(equation 5).

 doi:10.20944/preprints202504.0616.v1

$$C_{estimated(t)} = \frac{I_{estimated(t)} - I_{0(n)}}{a_{calibration(n)}} \quad (5)$$

3. Results

3.1. Electrochemical Properties of Nafion / GOD-BSA / Pt Biosensor

The basic performance of the Nafion / GOD-BSA / Pt biosensor was evaluated by amperometry measurements in DMEM containing 0-30 mM at fluidic conditions. The GOD molecule was known to catalyze the oxidization of glucose with molecular oxygen to gluconolactone and produce H2O2. Then, the oxidation of H2O2 was carried out at the Pt electrode, contributing to electron transfer. The concentration of glucose is related to the rate of both oxidation reactions [23,24]. The possible reaction mechanisms are as follows.

$$O_2 + glucose \xrightarrow{GOD} Gluconolactone + H_2O_2 \quad (6)$$

$$H_2O_2 \rightarrow 2H^+ + O_2 + 2e^- \quad (7)$$

As shown in Figure 3, the anodic current was dependent on glucose concentrations at the fluidic condition. The current response increased significantly and then gradually increased as the glucose concentration increased. According to the results, the Michaelis-Menten kinetic mechanism was used to exhibit the characteristics of the biosensor. The relationship between the current response and glucose concentration was expressed as the following Lineweaver-Burk type equation (equation 8) [25], which consists of the current (I), the glucose concentration (C), the apparent Michaelis-Menten constant (Kmapp), and the maximum anodic current (Imax).

$$\frac{1}{I} = \frac{K_m^{app}}{I_{max}}\left(\frac{1}{[C]}\right) + \frac{1}{I_{max}} \quad (8)$$

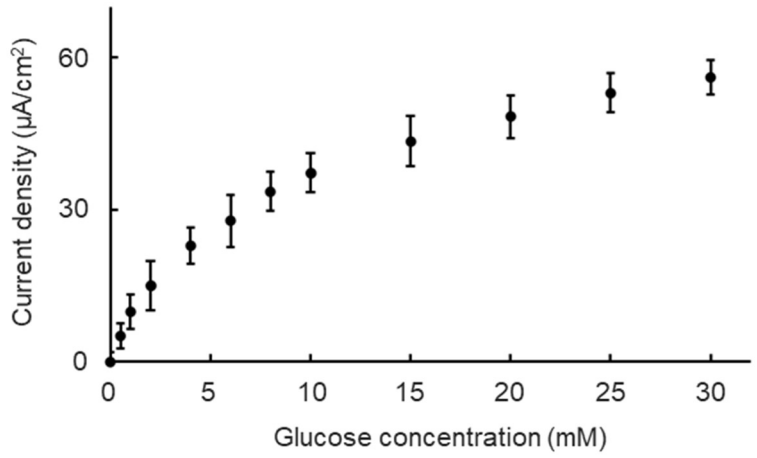

Figure 3. Biosensor outputting current density versus glucose concentration in DMEM (pH 7.4) at 37 °C. Values indicate mean ± standard deviation.

Based on the equation, the I_{max} and K_m^{app} were calculated about 44 μA/cm² and 2.9 mM, that indicated the biosensor has a basic function to detect the glucose at different concentrations. However, the obtained K_m^{app} value was lower than that for the free enzyme in solutions (33 mM) [26]. This result indicates that structural distortion due to attaching enzymes onto the substrate causes retardation of catalytic reaction rates, leading to the low value of K_m^{app}.

The glucose concentration range of 0 mM to 30 mM was divided into the low concentration range of 0 mM to 2 mM, the middle concentration range of 2 mM to 10 mM, and the high concentration range of 10 mM to 30 mM. Three ranges were divided to correspond to the glucose concentration of three types of universal culture medium: the no-glucose DMEM (0 mM glucose), the low-glucose DMEM (5.6 mM glucose), and the high-glucose DMEM (25 mM glucose). The sensitivities and resolutions of the biosensor at different ranges were quantified as a validation of the biosensor's basic

 doi:10.20944/preprints202504.0616.v1

performance. The calculated sensitivities and resolutions of the biosensor at different glucose concentration ranges are shown in Table 1. The sensitivity decreased, and the resolution increased as the glucose concentration range increased. However, deviations of sensitivities and resolutions at every glucose concentration range didn't show significant differences.

From the essential performance evaluation of experimental results, the biosensor performed well in fluid conditions. This indicates that the perfusion conditions create steady and constant glucose supplements, leading to a steady response current that contributes to higher sensitivity and detection ability (resolution). The glucose concentration's variation after the medium passed through the cell culture chamber was calculated using the following equation (equation 9), which consists of glucose concentration's variation (D_{cells}), the HepG2 cells' glucose consumption rate (GCR=4.1×10^{-16} mols^{-1}cell^{-1}) [27], Time for the culture medium to pass through the cell culture chamber (t=1770 s), the Total number of cells (N=10^6), and the volume of the cell culture chamber ($V_{chamber}$=265 μL).

$$D_{cells} = \frac{GCRtN}{V_{chamber}} \quad (9)$$

Based on the equation, the glucose concentration's variation was calculated at about 2,900 μM. Thus, the essential resolution that securing the glucose concentration changes can be monitored must be below 2,900 μM. Both biosensors' resolutions at high, mid, and low glucose ranges were achieved further than the required resolutions. The performance of the biosensor met the requirements of our platform.

3.2. Long-Term Monitoring of Constant Glucose Concentration

First, the flow distributions in the biosensor chamber were evaluated to confirm the object solution complete reaction at the working electrode and ensure the measurement's accuracy in the calibration phases. The flow rate distribution of the main inlet and two calibration solutions inlets was adjusted within a total flow rate of 9.0 μL/min to control the solutions distribution in the biosensor chamber. The solutions distribution changes were observed by stereo microscope (SMZ25, Nikon, Tokyo, Japan), using red and blue pigment solutions. The solutions distribution caused by flow rate distribution of 8.8:0.1:0.1 μL/min is shown in Figure 2B. The object solutions nearly fill the sensor chamber and cover the enzyme casting area in the following flow rate distribution.

Then, the long-term monitoring experiment was executed. The response current during the long-term monitoring within 20 h is shown in Figure 4A, slightly declined at a constant 5.6 mM glucose concentration, and the clear response current peak and feet appeared at each calibration process after every 2 h of monitoring. Real-time glucose concentrations in every measurement phase were calculated using the following calculating method (section 2.7), the result is shown in Figure 4B. Against a slightly lowering response current, the calculated real-time glucose concentration was maintained at nearly 5.6 mM, which conformed with measurement results from the glucose analyzer (GP-9, Analox Instruments, England, UK).

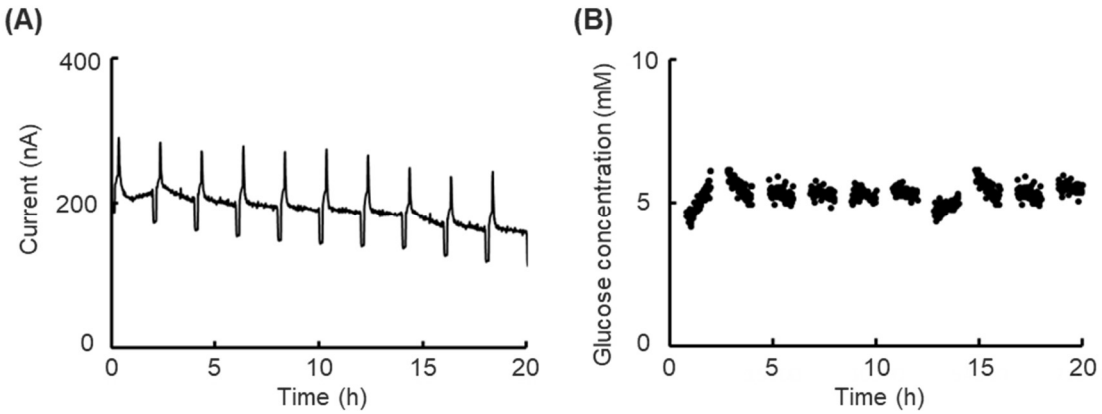

 doi:10.20944/preprints202504.0616.v1

Figure 4. Results of Long-term glucose concentration monitoring to evaluate calibration function without cells. (A) Time course of sensor response current in culture medium with low-glucose DMEM containing 5.6 mM glucose at 37°C with calibration function. (B) Time course of calculated glucose concentration using calibration data in culture medium with low-glucose DMEM containing 5.6 mM glucose at 37°C.

The biosensor's slight decline in response current can be considered the sensor's drift due to decreasing enzyme activity. The calculated real-time glucose concentration maintained at a consistent level, showed the calibration function is valid for certain predictions of glucose concentration. In enzyme-modified biosensors used in cell-based studies reported to date, the biosensor's drifts during the cell status monitoring were fixed by normalization with the control group [17]. However, the cell status difference between experimental groups will significantly influence the accuracy of cell drug toxicity experiments. In the other studies, the drifts were fixed by comparing the difference with glucose concentration at the inlet or outlet of a cell culture chamber [18]. However, any single biosensor will easily interfere with the experimental results. In this study, all discussions focus on one single biosensor, to avoid all external interference and inter-individual variabilities. The results showed the calibration function could eliminate the influence of biosensor drift during long-term monitoring and contributed to certain predictions of the objective's concentration. The glucose concentration in monitoring was maintained within near 5.6 mM, and non-forecast changes can be individually discussed. Furthermore, the calibration processes executed at intervals between every measurement process and the lack of a requirement to remove the platform from the incubator contribute to the continuousness of measurement. Thus, our platform is readily available for glucose concentration prediction and advanced cell status monitoring.

3.3. Long-Term Monitoring at Cell Toxicity Experiment

Paraquat, known as an international forbidden non-selective herbicide, leading to significant cell toxicity and DNA damage, was applied in the cell toxicity experiment [28–30]. The glucose concentration in the cell toxicity experiment was monitored to validate the usability of our platform at dynamic glucose concentration conditions. The response current during the cell toxicity experiments is shown in Figure 5A, the peaks of the response current from the calibration processes were observed every 2 h during the experiment. The response current level was clearly different depending on the paraquat dose, and a general downward drift phenomenon was observed. The calculated glucose consumption is shown in Figure 5B. The calculated glucose consumption was expressed as a moving average and normalized with the initial glucose consumption value. The group at culture conditions with 5 mM and 10 mM paraquat showed a significant decrease in glucose consumption within the first 7 h. After glucose consumption decreased, the glucose consumption of both groups exposed to paraquat tended to stabilize.

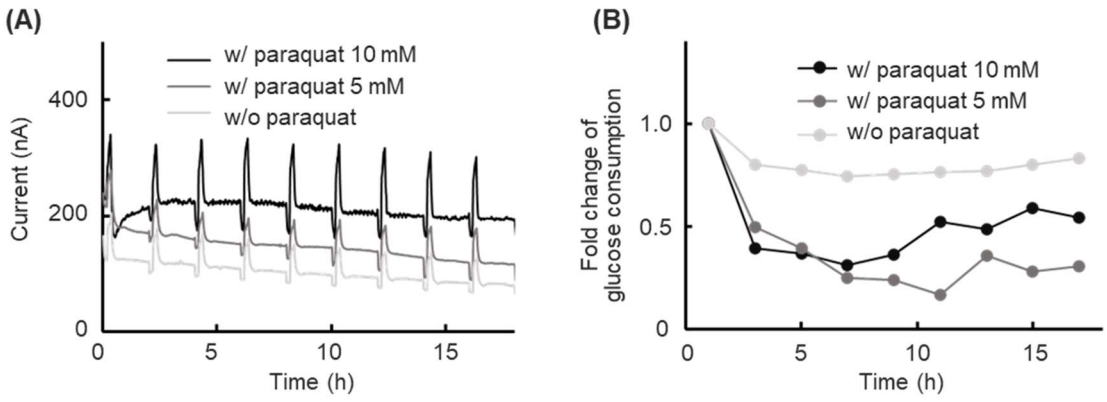

Figure 5. Results of long-term glucose concentration monitoring in a cell toxicity experiment. (A) Time course of sensor response current for cells without paraquat, cells with 5 mM paraquat, and cells with 10 mM paraquat in

 doi:10.20944/preprints202504.0616.v1

culture medium (low-glucose DMEM containing 5.6 mM glucose), with automatic calibration performed every 2 h. (B) Time course of the glucose consumption for cells without paraquat, cells with 5 mM paraquat, and cells with 10 mM paraquat in the culture medium, as determined by automatic calibration. Values indicate moving average. The relative glucose consumption value was normalized with the initial glucose consumption value.

In a previous study on paraquat toxicity to HepG2 cells, it was reported that cell viability significantly decreased as the paraquat concentration increased [31]. However, the cell assay in this previous study was non-continuous, and they were unable to obtain more detailed information during the paraquat exposure. In our study, the cell kinetic status changes were chronologically quantified evaluated by long-term monitoring of glucose consumption. Glucose consumption decreases leading by paraquat's cell toxicity was observed at our platform. From the results, our platform showed the usability of cell-based analysis and was expected to apply more cell experiments and studies. All cell status analysis and discussion focused on data measured by one single biosensor and compared with other conditions, contribute by calibration function making certain measurements possible to happen at one single biosensor. Moreover, all the experimental results proved our platform is more suitable for cell-based analysis in certain sections.

4. Conclusions

In this study, we presented a platform for the analysis of changes in cells' kinetic physiological conditions by integrating an enzyme-casting electrochemical biosensor to obtain real-time glucose consumption changes and apply it to cell toxicity experiments. The cell kinetic status changes were realized as glucose consumption changes, which were obtained by response current from the enzyme's oxidation-reduction reactions. The calibration functions were achieved by spatiotemporally controlling the glucose concentration of the cell culture medium and detecting the decline of current to calibrate the biosensor's drift. The long-term monitoring of the glucose level experiment demonstrated that glucose concentration could be accurately monitored over 20 h, providing a relative prediction of glucose concentration, which was contributed to by the calibration function. In the cell toxicity experiment, the toxicity of paraquat was observed on our platform, demonstrating that monitoring more detailed changes in cell kinetic status is possible. The results of the experiments show that our platform is suitable for cell-based assays, and more medical development studies are expected to be applied.

Author Contributions: Conceptualization: H.K.; Methodology: L.C., K.K., and H.K.; Validation: L.C, S.K., and H.N.; Formal analysis: L.C. and S.K.; Investigation: K.K. and H.K.; Writing—original draft: L.C. and S.K.; Writing—review & editing: K.K. and H.K.; Project administration: H.K.; Funding acquisition: H.K. All authors have read and agreed to the published version of the manuscript.

Funding: This work was partially supported by JSPS KAKENHI (Grant number JP18H01849).

Data Availability Statement: The original contributions presented in this study are included in the article. Further inquiries can be directed to the corresponding author.

Acknowledgments: We would like to thank Mr. Tomoki Suzuki for his support with device fabrication and the Tokai University Imaging Center for Advanced Research (TICAR) for their technical assistance.

Conflicts of Interest: The authors declare no conflict of interest.

References

1. Dongeun, H.; Yu-suke, T.; Geraldine, A. H.; Hyun, J. K.; Donald, E. I. Microengineered physiological biomimicry: organs-on-chips. *Lab on a Chip* 2012, 12, 2156–2164.
2. Kimura, H.; Sakai, Y.; Fujii, T. Organ/body-on-a-chip based on microfluidic technology for drug discovery. *Drug Metabolism and Pharmacokinetics* 2018, 33, 43–48.

 doi:10.20944/preprints202504.0616.v1

3. Sung, J. H.; Srinivasan, B.; Esch, M. B.; McLamb, W. T.; Bernabini, C.; Shuler, M. L.; Hickman, J. J. Using physiologically-based pharmacokinetic-guided "body-on-a-chip" systems to predict mammalian response to drug and chemical exposure. *Experimental biology and medicine* 2014, 239, 9, 1225-1239 .
4. Kimura, H.; Nishikawa, M.; Kutsuzawa, N.; Tokito, F.; Kobayashi, T.; Kurniawan, D.A.; Shioda, H.; Cao, W.; Shinha, K.; Nakamura, H.; Doi, K.; Sakai, Y. Advancements in microphysiological systems: exploring organoids and organ-on-a-chip technologies in drug development—focus on pharmacokinetics related organs. *Drug Metabolism and Pharmacokinetics* 2024, 101046.
5. Jun, Y.; Lee, J.S.; Choi, S.; Yang, J.H.; Sander, M.; Chung, S.; Lee, S.H. In vivo–mimicking microfluidic perfusion culture of pancreatic islet spheroids. *Science Advances* 2019, 5, 11, 1-13.
6. Ziółkowska, K.; Kwapiszewski, R.; Brzózka, Z. Microfluidic devices as tools for mimicking the in vivo environment. *New Journal Chemistry* 2011, 35, 979–990.
7. Huang, H.C.; Chang, Y.J.; Chen, W.C.; Tsai, C.H.; Chen, Y.H.; Chen, Y.C. Enhancement of renal epithelial cell functions through microfluidic-based coculture with adipose-derived stem cells. *Tissue Engineering Part A* 2013, 19, 17-18, 2024–2034.
8. Tahirbegi, I.B.; Ehgartner, J.; Sulzer, P.; Zieger, S.; Kasjanow, A.; Paradiso, M.; Strobl, M.; Bouwes, D.; Mayr, T. Fast pesticide detection inside microfluidic device with integrated optical pH oxygen sensors and algal fluorescence. Biosens. Bioelectron. 2017, 88, 15, 188–195.
9. Gonzalez-Guerrero, M.J.; Raboso-Gallego, T.; Fernandez-Sanchez, C.; de Marcos, S.; Lopez-Ruiz, B. Paper-based microfluidic biofuel cell operating under glucose concentrations within physiological range. *Biosensors and Bioelectronics* 2017, 90, 475–480 .
10. Kumar, P.; Nagarajan, A.; Uchil, P.D. Analysis of cell viability by the lactate dehydrogenase assay. *Cold Spring Harbor Protocols* 2018, 6.
11. Wong, C.M.; Wong, K.H.; Chen, X.D. Glucose oxidase: natural occurrence, function, properties and industrial applications. *Applied Microbiology and Biotechnology* 2008, 78, 927–938.
12. Iogr, A.; Schuhmann, W.; Huber, J. Enzyme electrodes to monitor glucose consumption of single cardiac myocytes in sub-nanoliter volumes. *Biosensors and Bioelectronics* 2010, 25, 5, 1019–1024.
13. Bollella, P.; Katz, E. Enzyme-based biosensors: tackling electron transfer issues. *Sensors* 2020, 20, 12, 3517.
14. O'Neill, D.; Chang, S.C.; Lowry, J.P.; McNeil, C.J. Comparisons of platinum, gold, palladium and glassy carbon as electrode materials in the design of biosensors for glutamate. *Biosensors and Bioelectronics* 2004, 19, 11, 1521–1528.
15. Komori, K.; Komatsu, Y.; Nakane, M.; Sakai, Y. Bioelectrochemical detection of histamine release from basophilic leukemia cell line based on histamine dehydrogenase-modified cup-stacked carbon nanofibers. *Bioelectrochemistry* 2021, 138, 107719.
16. Sekhwama, M.; Mpofu, K.; Sudesh, S.; Mhlanga, S. Integration of microfluidic chips with biosensors. *Discover Applied Sciences* 2024, 6, 458.
17. Kimura, H.; Takeyama, H.; Komori, K.; Yamamoto, T.; Sakai, Y.; Fujii, T. Microfluidic device with integrated glucose sensor for cell-based assay in toxicology. *Journal of Robotics and Mechatronics* 2010, 22, 5, 594–600.
18. Kimura, H.; Shono, Y.; Pereira-Rodrigues, N.; Yamamoto, T.; Sakai, Y.; Fujii, T. On-chip glucose sensor for online measurement of cell activities. *IEEJ Transactions on Sensors and Micromachines* 2010, 130, 476–483.
19. Tanaka, Y.; Yamato, M.; Okano, T.; Kitamori, T.; Sato, K. Evaluation of effects of shear stress on hepatocytes by a microchip-based system. *Measurement Science and Technology* 2006, 17, 3167.
20. Hosokawa, K.; Fujii, T.; Endo, I. Handling of picoliter liquid samples in a poly(dimethylsiloxane)-based microfluidic device. *Analytical Chemistry* 1999, 71, 20, 4781–4785.
21. Fortier, G.; Vaillancourt, M.; Bélanger, D. Evaluation of nafion as media for glucose oxidase immobilization for the development of an amperometric glucose biosensor. *Electroanalysis* 1992, 4, 3, 275–283.
22. Rishpon, J.; Gottesfeld, S.; Campbell, C.; John, D.; Thomas A.Z.Jr. Amperometric glucose sensors based on glucose oxidase immobilized in nafion. *Electroanalysis* 1994, 6, 1, 17–21.
23. Bankar, S.B.; Bule, M.V.; Singhal, R.S.; Ananthanarayan, L. Glucose oxidase—an overview. *Biotechnology Advances* 2009, 27, 4, 489–511.
24. Mandpe, P.; Prabhakar, B.; Gupta, H.; Shende, P. Glucose oxidase-based biosensor for glucose detection from biological fluids. *Sensor Review* 2020, 40, 4, 497–511.

 doi:10.20944/preprints202504.0616.v1

25. Kamin, R.A.; Wilson, G.S. Rotating ring-disk enzyme electrode for biocatalysis kinetic studies and characterization of the immobilized enzyme layer. *Analytical Chemistry* 1980, 52, 8, 1198–1205.
26. Swoboda, B.E.P.; Massey, V. Purification and properties of the glucose oxidase from Aspergillus niger. *Journal of Biological Chemistry* 1965, 240, 5, 2209–2217.
27. Shirakashi, R.; Yoshida, T.; Provin, C.; Sato, K.; Funamoto, K.; Takahashi, M.; Hibino, T.; Takiguchi, T. Steady measurement of glucose metabolism of hepatocyte. In Proceedings of the Heat Transfer Summer Conference, Vancouver, Canada, July 2007; ASME: New York, NY, USA, 2007; Paper No. 42762, 65–70.
28. Teixeira, H.; Proença, P.; Alvarenga, M.; Oliveira, M.; Marques, E.P. Vieira, D.N. Pesticide intoxications in the centre of Portugal: three years analysis. *Forensic Science International* 2004, 143, 2-3, 199–204.
29. Urbančíková, M.; Korytár, P. Cu-complex counteracts the effect of paraquat on polymerized actin. *Toxicology* in Vitro 1999, 13, 4-5, 785–788.
30. Lee, D.Y.; Kang, H.W.; Kaneko, S.; Kwon, Y.S.; Muramatsu, H. Direct monitoring of paraquat induced cell death using quartz crystal sensor. *Thin Solid Films* 2009, 518, 2, 707–710.
31. Vrzal, R.; Zenata, O.; Doricakova, A.; Dvorak, Z. Environmental pollutants parathion, paraquat and bisphenol A show distinct effects towards nuclear receptors-mediated induction of xenobiotics-metabolizing cytochromes P450 in human hepatocytes. *Toxicology Letters* 2015, 238, 1, 43–53.